



## A new Online Hall Effect Sensor Fault Detection and Location in Brushless DC Motor Based on Normalized Phases Currents Analysis

M. Arehpanahi\*, M. Zare Ravandy

Department of Electrical Engineering, Tafresh University, Tafresh, Iran

### PAPER INFO

#### Paper history:

Received 16 May 2023

Received in revised form 15 September 2023

Accepted 19 September 2023

#### Keywords:

Brushless DC Motor

Fault Detection

Hall Sensor Fault

Normalized Current

Online Location

### ABSTRACT

In this paper, a new online technique for Hall Effect sensor fault diagnosis in brushless DC (BLDC) motor is proposed. The proposed technique is based on phase current waveform analysis and does not need any Hall sensor information. The normalized phases current values are analyzed per and post-sensor fault in every cycle. Using a definition of suitable conditions and threshold values for normalized currents values, all sensor fault types (i.e. set to 0 and 1) could be detected and located online effectively. The main contribution of this paper is introducing an online BLDC sensor fault detection and location technique under low-speed operation and transient conditions. Simulation results show the effectiveness of the proposed technique in all of the sensor faults types diagnosis without any sensor output value information. Two different types of BLDC motors are considered for fault diagnosis using the proposed technique. Simulation results during starting and low-speed operations of BLDC motor are well confirmed by the experimental results.

doi: 10.5829/ije.2023.36.12c.02

### NOMENCLATURE

$V_{dc}$	DC link voltage (V)	T	Period (s)
$R_s$	Stator resistance (Ohm)	n	Normalized value
$L_l$	Stator leakage inductance (H)	$S_{1,2,3,4,5,6}$	Power Switches
		$I_{A,B,C}$	Phases current

## 1. INTRODUCTION

High efficiency, high torque density, low-level noise, and wide speed control range are the main benefits of BLDC motors related to the induction motors. Therefore, BLDC motors can be one of the best options for many applications, such as robots, electric bicycles, and computer equipment [1-3]. But torque ripple [3, 4] and dependency on the rotor position are the main drawbacks of the BLDC motors. The switching pattern of a BLDC motor driver for speed control is highly dependent on the position sensors output values. The most common BLDC motor position sensors are Hall Effect sensors. These sensors may be damaged during operation of BLDC motors which can cause serious damage to the motor. Therefore, using an online sensor fault and driver faults

diagnosis technique is very important for the safe operation of the BLDC motor. There are many diagnosis techniques for detection of the sensor faults in BLDC motors. The sensor fault is detected based on the sum of the instantaneous of Hall output signal values with an investigated diagnosis table reported in literatu [5]. Cheshta et al. [5] focussed on the analysis of the output values of hall sensors for detection of faulty sensor. A new technique based on a binary combination of Hall signals values and commutation times between power switches of the BLDC driver is presented by Qian, and Ming [6]. A direct redundancy- based method by utilizing redundant Hall-effect sensors for Fault Tolerant Control (FTC) of a BLDC motor is presented by Aqil and Hur [7]. The online sensor fault diagnosis of BLDC motor are carried out by wavelet package [8], Goertzel

\*Corresponding author email: [arehpanahi@tafreshu.ac.ir](mailto:arehpanahi@tafreshu.ac.ir)  
(M. Arehpanahi)

Algorithm [9] and improved ZOA (Zeroth Order Algorithm) technique [10]. The DC-link current second harmonic component monitoring is employed for sensor fault diagnosis [11]. Mehta et al. [12] used analysis of the output sensor signals values sequences as binary numbers, the sensor faults can be detected. In healthy conditions, the sequence of three Hall-Effect sensors values (0 for OFF state and 1 for ON state) is expressed as one of the six binary numbers (from 001 to 110). Therefore, any sequences outside this range will be detected as a fault [13, 14]. No-detection at low-speed operation, is the main drawback of the mentioned techniques. Tashakori and Ektesab [13] analyzed the output sensor waveform based on reference frame theory and Vector-Tracking Observer (VTO) is employed for detection of faults especially at low-speed operation. But complex calculation process and requiring a rotating harmonic vectors models, are the main disadvantages of work reported in literature [15]. A new technique based on line-voltage monitoring using FFT analysis was proposed by Donato et al. [16]. Detection process complexity and no- detection during start-up are the main disadvantages of it. An improved FTC scheme based on FDP (Fault Detection Probability) and VTO for sensor fault diagnosis was proposed by Donato et al. [17]. No-fault detection during start-up is the main drawback of the reported data [15]. Diagnosis of Hall-Effect sensors faults based on output sensors signals values combined with the measured line voltages using Discrete Fourier Transform (DFT) was reported by Mousmi et al. [18]. Analysis of the stator phase currents using Stockwell Transform (S-Transform) for hall sensors faults diagnosis was defined by Gowtham et al. [19]. In general, no-fault detection at low-speed operation or false diagnosis in transient conditions is two challenges of the mentioned techniques. The inability to separate between starting and fault conditions is a main drawback of the most online sensor fault diagnosis techniques. If any sensors fail, they will affect on the stator current waveform directly. The stator current monitoring is a usual and accessible technique for analysis of the motor behavior. Therefore, in this paper, a new online technique based on phase current waveform analysis is proposed. In

the proposed technique, using all phases' current waveforms analysis, the sensor fault can be detected and located effectively. The main contribution of the proposed technique is definition of some conditions for normalized three phase currents values with a simple calculation process. The proposed technique, can able to separate transient conditions from fault conditions. This paper is divided into four sections: section 1 proposed method, section 2 simulation results and discussion, section 3 experimental results and section 4 conclusion.

## 2. PROPOSED METHOD

Usually, during sensor failure time, the output value of the sensor is unchanged (0 or 1). Therefore, in this paper, a constant value of the sensor output is considered as a fault. Figure 1 shows a block diagram of the BLDC motor driver which is used in this paper. Table 1 shows the switching pattern of the BLDC motor driver under sensor A fault (set to 0). If a sensor output value is to be constant, the status of some switches will be always ON or OFF. Then, in half of the period (positive or negative) the corresponding phase current is close to zero. According to Table 1, in a period, it is clear that  $I_A$  has positive and negative signs but  $I_B$  has negative sign and  $I_C$  has positive sign. Therefore,  $I_C$  and  $I_B$  have a DC component. If this DC component pre and post-fault is well analyzed, the sensor fault could be well detected. DC component of phase currents affects on the average and RMS value of the phase current.

Therefore, in the proposed technique, the average value of the phase current divided by the RMS value of that which is called normalized phase current, is introduced as a fault indicator. The normalized phase current value is expressed in Equation (1):

$$I_{xn} = \frac{1}{T I_{Nrms}} \int_t^{t+T} I_x dt \quad x = A, B, C \quad (1)$$

where  $T$ ,  $I_{Nrms}$   $n$  are a period, nominal RMS value of phase current and the normalized value, respectively. In healthy conditions, the average value of all phase

**TABLE 1.** Switching pattern of BLDC motor driver under sensor A fault (logic 0)

State	Hall Effect sensor status			Active switches	Phase currents sign		
	A	B	C		A	B	C
1	0	0	1	S1,6	positive	negative	none
2	0	0	1	S1,6	positive	negative	none
3	0	0	0	none	none	none	none
4	0	1	0	S5,4	negative	none	positive
5	0	1	0	S5,4	negative	none	positive
6	0	1	1	S5,6	none	negative	positive

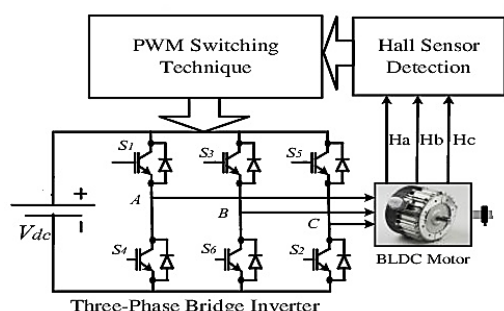


Figure 1. Three- phase BLDC motor driver

currents is close to zero. If one of the hall sensors (set to 0 or 1), the average value of all phase current will not be zero anymore. In this condition, according to Table 1, the positive or negative half period of phase current (depended on the sensor number failure) is close to zero approximately. Therefore, the absolute value of the corresponding phase current average will be about 50% of phase current RMS value. Therefore, according to Equation (1), the absolute normalized value of corresponding phases is close to 0.5. then using comparison of the mentioned normalized value with threshold value (i.e. 0.5), the sensor fault can be detected. However, the main problem in fault detection process, is normalized current variation during transient conditions (for example: starting time). To solve this problem, several simulations of different three-phase BLDC motors types (different output powers) during starting time are done. By analysing their results (variation of the all phase normalized currents values), it was found that the absolute normalized phase currents values are no higher than 0.4. Therefore, it can be defined suitable conditions for the normalized phase currents with an appropriate threshold value i.e. 0.4 (which is independent of BLDC motor specification) for fault indicator. The proposed technique, for detection and location of Hall-Effect sensors failure is expressed as six conditions in Tables 2 and 3(for two faults type). The subscript “n” denotes the normalized value.

For example, when three phase normalized currents satisfy in  $I_{An} < 0, I_{Bn} < -0.4, I_{Cn} > 0.4$ , based on Table 2, the sensor A has failed and set to 0. In diagnosis process, some problems may negatively impact on the fault detection such as rotation direction change, transient

TABLE 2. sensor fault diagnosis (logic 0)

Defective Sensor	Normalized phase current states
A	$I_{An} < 0, I_{Bn} < -0.4, I_{Cn} > 0.4$
B	$I_{An} > 0.4, I_{Bn} < 0, I_{Cn} < -0.4$
C	$I_{An} < -0.4, I_{Bn} > 0.4, I_{Cn} < 0$

TABLE 3. sensor fault diagnosis (logic 1)

Defective Sensor	Phase currents
A	$I_{An} > 0, I_{Bn} > 0.4, I_{Cn} < -0.4$
B	$I_{An} < -0.4, I_{Bn} > 0, I_{Cn} > 0.4$
C	$I_{An} > 0.4, I_{Bn} < -0.4, I_{Cn} > 0$

conditions and low-speed operation. The impacts of these problems on the proposed technique are discussed in this paper. The rotation direction of three-phase BLDC motor is reversed by a shifting any two phases from three phases of the terminal voltages. Therefore, by exchanging only two rows in Table 2 or Table 3, it can be used these tables for reverse rotation direction. Consequently, any change in rotation direction does not effect on the proposed technique results at all. The second problem is transient conditions such as starting. In the proposed technique, this problem has been fixed by selecting 0.4 as a threshold value for the fault indicators. The normalized phase currents values in transient condition do not satisfy in conditions that are expressed in Table 2 or Table 3 with this threshold value.

### 3. SIMULATION RESULTS AND DISCUSSION

In order to performance analysis of the proposed technique, two BLDC motors types (motors 1 and 2) with different specifications are considered. The specifications of both motors are listed in Tables 4 and 5.

Both motors (motors 1 and 2) have been started under different load conditions (no-load and full-load). Then sensor faults (logic 0 and logic 1) have been applied to all sensors individually when motors reach steady-state conditions. All simulation results have been done in MATLAB/Simulink software. For example, in motor 1, the fault (logic 0) is applied to the sensor A under full

TABLE 4. BLDC motor1 specification

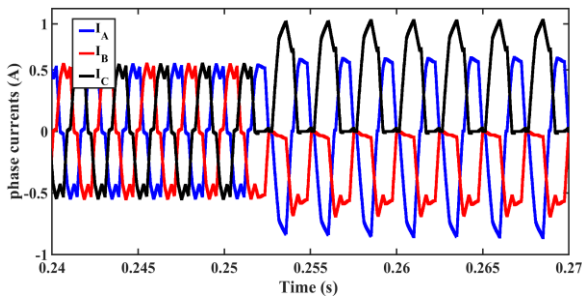
Parameter	Value	Parameter	Value
$V_{dc}$	48 V	Poles	4
$R_s$	0.28Ω	Rated power	200 W
$L_l$	0.45mH	Rated Speed	4000 rpm

TABLE 5. BLDC motor2 specifications

Parameter	Value	Parameter	Value
$V_{dc}$	48 V	Poles	4
$R_s$	0.069Ω	Rated power	1500 W
$L_l$	0.2mH	Rated Speed	5000 rpm

load conditions at time  $t=0.255$  s (Figures 2 and 3). For motor 2, another sensor fault type (logic 1) is applied to sensor B, under no load conditions at time  $t=0.25$  s (Figures 4 and 5). The phase current waveforms and their normalized values waveforms for motor 1 under full load pre and post-fault are illustrated in Figures 2 and 3. According to Figure 3 ( $I_{An} < 0, I_{Bn} < -0.4, I_{Cn} > 0.4$ ) and based on row 1 from Table 2 it is clear that the sensor A has failed (logic 0). The phase currents waveforms for motor 2, under no load pre and post-fault are shown in Figures 4 and 5. According to Figure 5 ( $I_{An} < -0.4, I_{Bn} > 0, I_{Cn} > 0.4$ ) and based on row 2 from Table 3, sensor B has failed (logic 1). Therefore, the proposed technique could detect and locate sensor fault.

The normalized phase currents values of motor1 under no-load, during starting time is illustrated in Figure 6. During starting time  $0.015s < t < 0.018s$  based on Figure



**Figure 2.** Phase currents of motor1 under full load and sensor A fault (logic 0)

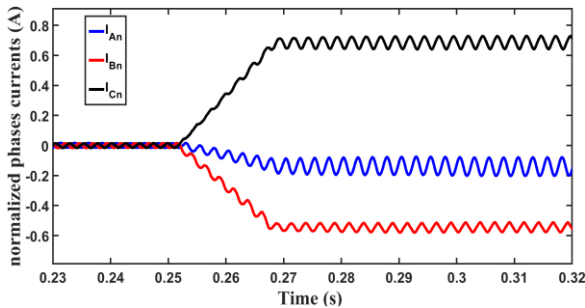


**Figure 3.** Normalized phase currents of motor1 under full load and sensor A fault (logic 0)

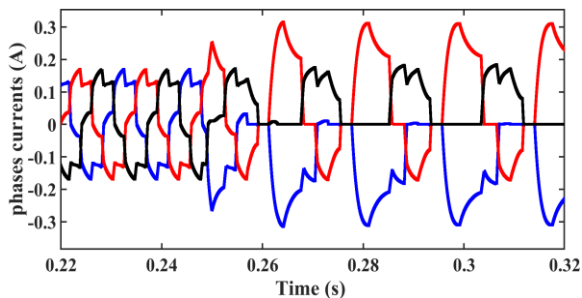


**Figure 4.** Phase currents of moto 2 under no-load and sensor B fault (logic 1)

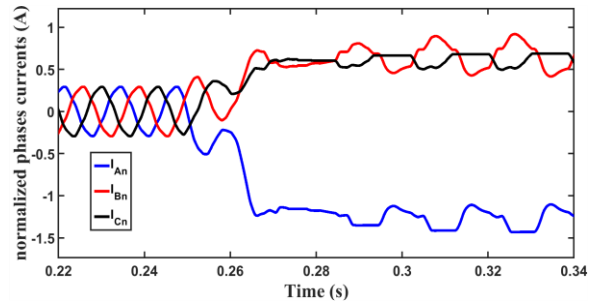


**Figure 5.** Normalized phase currents of moto 2 under no-load and sensor B fault (logic 1)

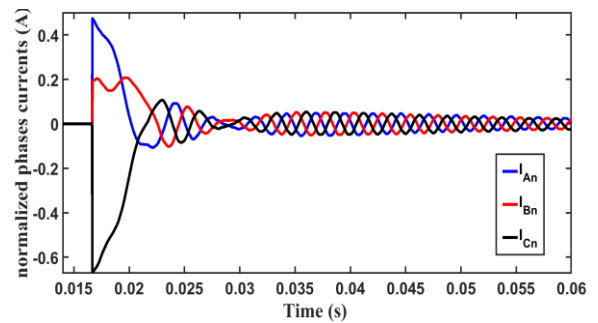


**Figure 6.** Normalized phase currents of motor 1 (starting)

6, the normalized phase currents values satisfy in  $I_{An} > 0.4, I_{Bn} > 0, I_{Cn} < -0.4$ .

As a result, motor 1 normalized current values during start-up do not satisfy in Tables 2 and 3 conditions. Consequently, the proposed technique is robust against transient conditions, especially during start-up. At low-speed operation, the phase current waveforms are changed related to the normal speed and contain low order harmonics. These waveforms are similar to the faulty cases. The sensor fault (sensor C, logic 1) is applied to motor 1 at 300 rpm (7.5% of rated speed). The sensor fault (sensor B, logic 1) is applied to motor 2 at 250 rpm (5% of rated speed). The phase current waveforms and their normalized values of motor 1 pre and post-fault are shown in Figures 7 and 8. The phase current waveforms and their normalized values of motor 2 pre and post-fault are shown in Figures 9 and 10.

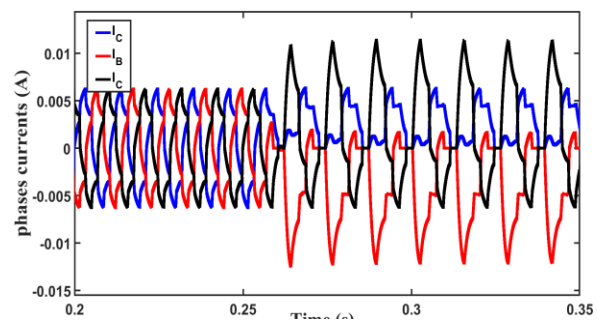


**Figure 7.** Phase currents (motor 1) at low speed (300 rpm)

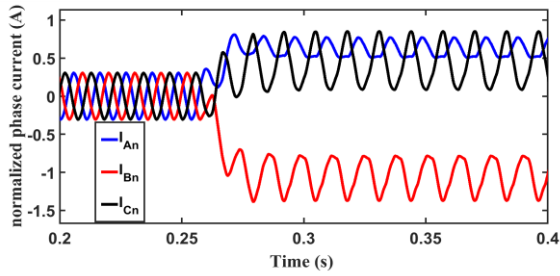


**Figure 8.** Normalized phase currents (motor 1) at low speed (300 rpm)

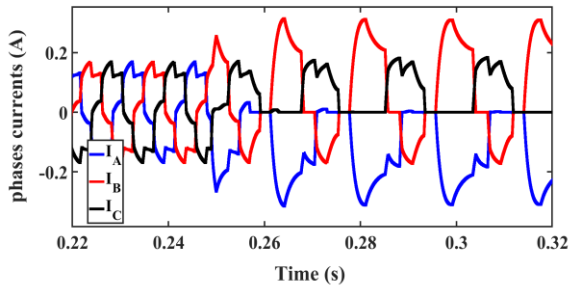


**Figure 9.** Phase currents (motor 2) at low speed (250 rpm)

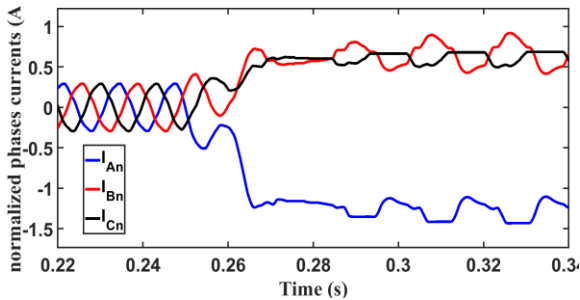


**Figure 10.** Normalized phase currents (motor 2) at low speed (250 rpm)

According to Figure 8, it is clear that the normalized phase current values of motor 1 in post- fault time are  $I_{An} > 0.4, I_{Bn} < -0.4, I_{Cn} > 0$  which satisfies in row 3 in Table 3. Therefore, sensor C has failed (logic 1). Also, the normalized phase currents values of motor2 (Figure 10) in post-fault time are  $I_{An} < -0.4, I_{Bn} > 0, I_{Cn} < 0.4$  which satisfies in row 2 in Table 3. Consequently, sensor B has failed (logic 1). Therefore, the proposed technique could online detect and locate all of the Hall-Effect sensor faults types in transient conditions, no- load, full-load and low-speed operation effectively.

**4. EXPERIMENTAL RESULTS**

In order to experimentally verify the proposed technique, a prototype BLDC motor is considered (Figure 11). The

prototype BLDC motor is designed for analysis of the motor under sensor fault conditions. In other words, the motor driver software is designed to be able to apply sensor faults. Specification of the prototype BLDC motor is listed in Table 6. The BLDC motor starts under no-load conditions. In steady-state conditions, sensor A is disconnected from the driver at  $t=0.4s$  (logic 0). Three-phase currents pre and post fault is illustrated in Figures 12, 13 and 14.

According to the phase currents waveforms and the normalized phase currents which are shown in Figures 15, 16 and 17, the normalized phases currents satisfy in

**TABLE 6.** BLDC motor specification for testing

Parameter	Value	Parameter	Value
$V_{dc}$	24 V	Nominal current	2.32 A
$R_s$	0.5 $\Omega$	Rated torque	83 mNm
$L_l$	0.55mH	Rated Speed	5250 rpm



**Figure 11.** Set-up of the prototype BLDC motor

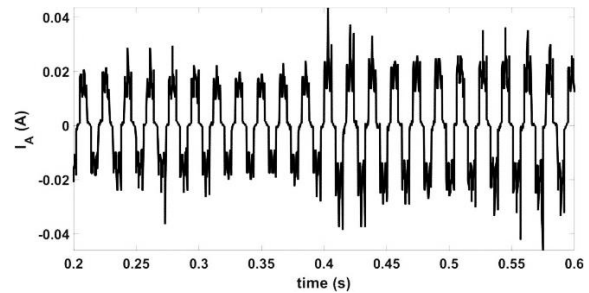


**Figure 12.** Phase A current waveform pre and post fault

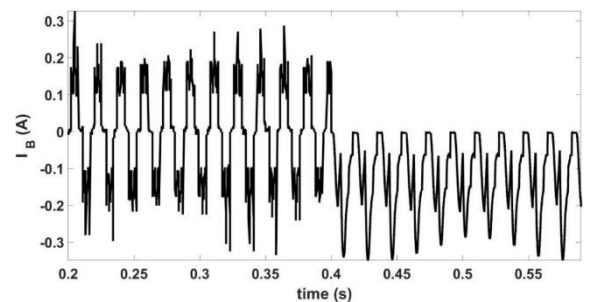


**Figure 13.** Phase B current waveform pre and post fault

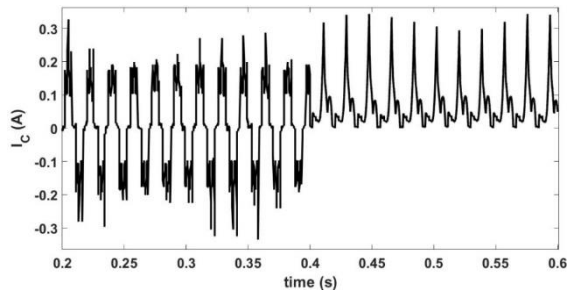


Figure 14. Phase C current waveform pre and post fault

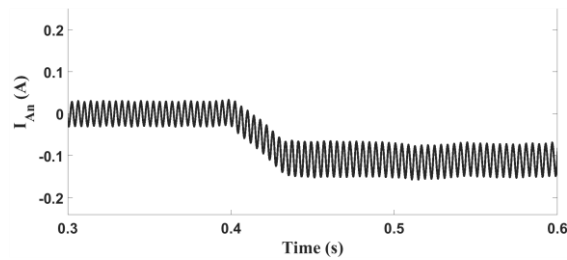


Figure 15. Normalized of I<sub>A</sub> waveform pre and post fault

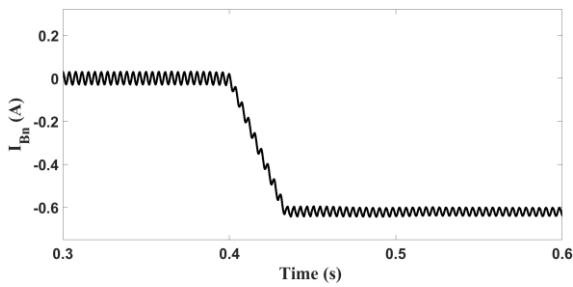


Figure 16. Normalized of I<sub>B</sub> waveform pre and post fault

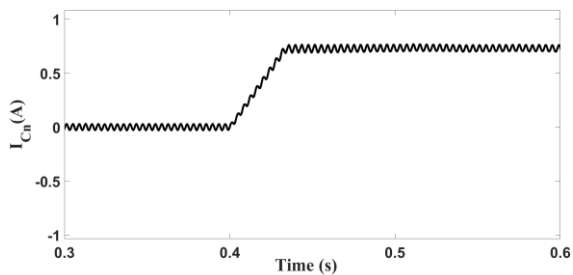


Figure 17. Normalized of I<sub>c</sub> waveform pre and post fault

$I_{An} < 0, I_{Bn} < -0.4, I_{Cn} > 0.4$ . Therefore, based on row 1 in Table 2, sensor A is failed (logic 0).

To analysis of the proposed technique under low-speed operations, the prototype BLDC motor operates at low- speed i.e. 250 rpm. The sensor fault is applied to the sensor A (logic 0) at  $t=0.43s$ . The three phase currents of the BLDC motor are illustrated in Figures 18, 19 and 20. The normalized value of three phase currents are illustrated in Figures 21, 22 and 23. According to these figures, the normalized phase currents satisfy in  $I_{An} <$

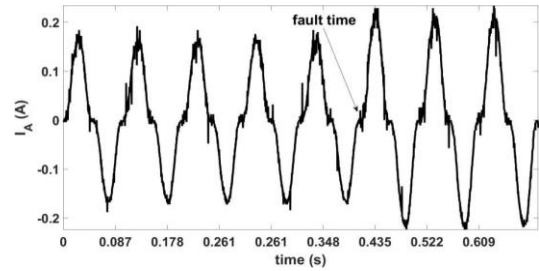


Figure 18. I<sub>A</sub> waveform pre and post fault (250 rpm)

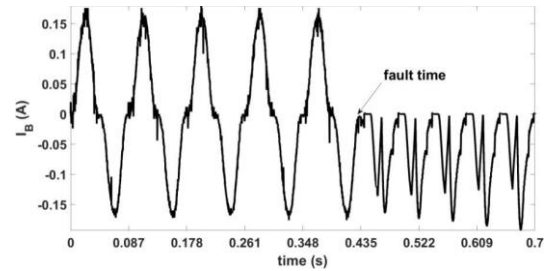


Figure 19. I<sub>B</sub> waveform pre and post fault (250 rpm)

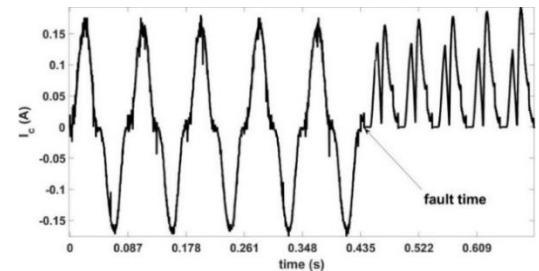


Figure 20. I<sub>c</sub> waveform pre and post fault (250 rpm)

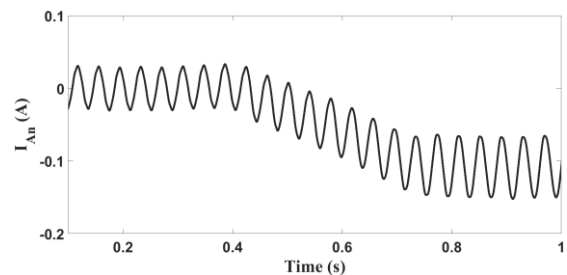


Figure 21. Normalized I<sub>A</sub> waveform pre and post fault (250 rpm)

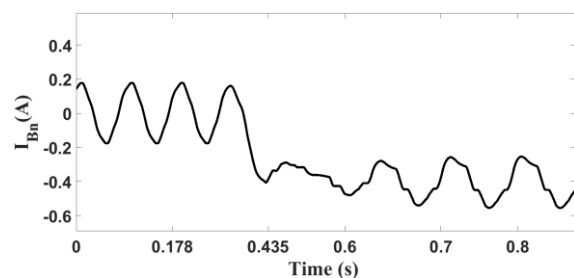
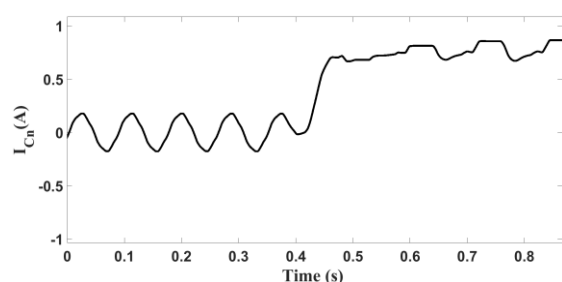


Figure 22. Normalized I<sub>B</sub> waveform pre and post fault (250 rpm)



**Figure 23.** Normalized  $I_C$  waveform pre and post fault (250 rpm)

$0, I_{Bn} < -0.4, I_{Cn} > 0.4$ . As a result, based on row 1 in Table 2, the sensor A is failed (logic 0). Consequently, the proposed technique could detect and locate online all of the sensor faults types at different operation conditions.

## 5. CONCLUSION

This paper presents a new online detection technique for Hall-Effect sensor faults in brushless DC motors. In the proposed technique, the sensor fault is detected and located online by the normalized phase currents analysis. The proposed technique is also able to detect sensor faults at low speeds. Using a comparison of all normalized phases current values with suitable threshold value, the sensor fault (type and sensor number) is detected and located effectively. The proposed technique, can separate transient conditions such as starting from faulty cases which is the main advantage of the proposed technique related to the other diagnosis techniques. The simulation results for two different types of the BLDC motors under different loads and speed conditions, show the capability of the proposed technique in sensor fault diagnosis. Verification of the proposed technique is carried out by experimental results effectively.

## 6. REFERENCES

- Procter, S. and Secco, E.L., "Design of a biomimetic bldc driven robotic arm for teleoperation & biomedical applications", *J Hum Earth Future. ISSN*, (2022), 2785-2997. doi: 10.28991/HEF-2021-02-04-03.
- Morales, L.A., Fabara, P. and Pozo, D.F., "An intelligent controller based on lamda for speed control of a three-phase inductor motor", *Emerging Science Journal*, Vol. 7, No. 3, (2023), 676-690. doi: 10.28991/ESJ-2023-07-03-01.
- Patel, A. and Suthar, B., "Cogging torque reduction of sandwiched stator axial flux permanent magnet brushless dc motor using magnet notching technique", *International Journal of Engineering, Transactions A: Basics* Vol. 32, No. 7, (2019), 940-946. doi: 10.5829/IJE.2019.32.07A.06.
- Gol, S., Ardeshir, G., Zahabi, M. and Ale Ahmad, A., "The influence of dc-link voltage on commutation torque ripple of brushless dc motors with two-segment pulse-width modulation control method", *International Journal of Engineering, Transactions B: Applications* Vol. 31, No. 2, (2018), 307-314. doi: 10.5829/ije.2018.31.02b.15.
- Jain, C., Garg, P. and Jain, A.K., "Hall-effect sensor fault diagnosis, identification and remedial strategy in permanent magnet brushless dc drive", in 2018 IEEE International Conference on Power Electronics, Drives and Energy Systems (PEDES), IEEE. (2018), 1-5.
- Zhang, Q. and Feng, M., "Fast fault diagnosis method for hall sensors in brushless dc motor drives", *IEEE Transactions on Power Electronics*, Vol. 34, No. 3, (2018), 2585-2596. doi: 10.1109/TPEL.2018.2844956.
- Aqil, M. and Hur, J., "A direct redundancy approach to fault-tolerant control of bldc motor with a damaged hall-effect sensor", *IEEE Transactions on Power Electronics*, Vol. 35, No. 2, (2019), 1732-1741. doi: 10.1109/TPEL.2019.2917559.
- Mitronikas, E., Papathanasopoulos, D., Athanasiou, G. and Tsotoulidis, S., "Hall-effect sensor fault identification in brushless dc motor drives using wavelets", in 2017 IEEE 11th International Symposium on Diagnostics for Electrical Machines, Power Electronics and Drives (SDEMPED), IEEE. (2017), 434-440.
- Papathanasopoulos, D.A., Spyropoulos, D.V. and Mitronikas, E.D., "Fault diagnosis of misaligned hall-effect position sensors in brushless dc motor drives using a goertzel algorithm", in 2019 IEEE 12th international symposium on diagnostics for electrical machines, power electronics and drives (SDEMPED), IEEE. (2019), 167-173.
- Skóra, M., "Operation of pm bldc motor drives with faulty rotor position sensor", in 2017 International Symposium on Electrical Machines (SME), IEEE. (2017), 1-6.
- Papathanasopoulos, D.A., Spyropoulos, D.V., Mitronikas, E.D. and Karlis, A.D., "Commutation angle self-calibrating technique for brushless dc motor drives with defective hall-effect position sensors", in 2020 International Conference on Electrical Machines (ICEM), IEEE. (2020), 1301-1307.
- Mehta, H., Thakar, U., Joshi, V., Rathod, K. and Kurulkar, P., "Hall sensor fault detection and fault tolerant control of pmsm drive system", in 2015 International Conference on Industrial Instrumentation and Control (ICIC), IEEE. (2015), 624-629.
- Tashakori, A. and Ektesabi, M., "A simple fault tolerant control system for hall effect sensors failure of bldc motor", in 2013 IEEE 8th Conference on Industrial Electronics and Applications (ICIEA), IEEE. (2013), 1011-1016.
- Dong, L., Jatskevich, J., Huang, Y., Chapariha, M. and Liu, J., "Fault diagnosis and signal reconstruction of hall sensors in brushless permanent magnet motor drives", *IEEE Transactions on Energy Conversion*, Vol. 31, No. 1, (2015), 118-131. doi: 10.1109/TEC.2015.2459072.
- Scelba, G., De Donato, G., Pulvirenti, M., Capponi, F.G. and Scarcella, G., "Hall-effect sensor fault detection, identification, and compensation in brushless dc drives", *IEEE Transactions on Industry Applications*, Vol. 52, No. 2, (2015), 1542-1554. doi: 10.1109/TIA.2015.2506139.
- Scelba, G., De Donato, G., Scarcella, G., Capponi, F.G. and Bonaccorso, F., "Fault-tolerant rotor position and velocity estimation using binary hall-effect sensors for low-cost vector control drives", *IEEE Transactions on Industry Applications*, Vol. 50, No. 5, (2014), 3403-3413. doi: 10.1109/TIA.2014.2304616.
- Dong, L., Huang, Y., Jatskevich, J. and Liu, J., "Improved fault-tolerant control for brushless permanent magnet motor drives with defective hall sensors", *IEEE Transactions on Energy Conversion*, Vol. 31, No. 2, (2016), 789-799. doi: 10.1109/TEC.2016.2526621.
- Mousmi, A., Abbou, A. and El Houm, Y., "Binary diagnosis of hall effect sensors in brushless dc motor drives", *IEEE*

*Transactions on Power Electronics*, Vol. 35, No. 4, (2019), 3859-3868. doi: 10.1109/TPEL.2019.2934794.

Energy, Systems and Information Processing (ICESIP), IEEE. (2019), 1-6.

19. Gowtham, S., Keerthana, I. and Balaji, M., "Characterization and classification of hall sensor faults using s-transform analysis on bldc motor drive", in 2019 IEEE 1st International Conference on

#### COPYRIGHTS

©2023 The author(s). This is an open access article distributed under the terms of the Creative Commons Attribution (CC BY 4.0), which permits unrestricted use, distribution, and reproduction in any medium, as long as the original authors and source are cited. No permission is required from the authors or the publishers.



---

#### Persian Abstract

چکیده

در این مقاله یک روش برخط جدید برای تشخیص خطای سنسور اثر هال در موتور DC بدون جاروبک پیشنهاد شده است. در روش پیشنهادی تحلیل شکل موج جریان فاز جایگزین بررسی خروجی حسگرهای موقعیت شده است. مقادیر جریان فازهای نرمال شده قبل و بعد از خطا در هر سیکل تجزیه و تحلیل می شوند. با استفاده از تعریف شرایط و مقادیر آستانه مناسب، همه انواع خطاهای حسگر می توانند به طور موثر و برخط شناسایی شده و محل خطا تعیین گیرند. مهمترین بخش مقاله تشخیص برخط خطای سنسور و مکان یابی آن در سرعت پایین است. نتایج شبیه سازی اثربخشی روش پیشنهادی را در تشخیص همه انواع خطاهای حسگر بدون استفاده مستقیم از مقدار خروجی سنسور نشان می دهد. دو نوع مختلف از موتورهای BLDC در شبیه سازی شده اند. نتایج شبیه سازی در شرایط کارکرد معمولی و سرعت پایین به خوبی توسط نتایج تجربی تایید شده اند.

---